Spherical Modal Filtering of Antenna Patterns Augmented by Translation of Coordinate Origin

Doren W. Hess
MI Technologies
Suwanee, GA, USA
dhess@mi-technologies.com

***Abstract*— This paper describes a novel method termed the *Isofilter*™ Technique, of isolating the radiation pattern of an individual radiator from among a composite set of radiators that form a complex radiation distribution. This technique proceeds via three successive steps: A spherical transform on an over-sampled data set, followed by a change of coordinate system followed in turn by filtering in the domain of the spherical modes to isolate a radiating source. The result is an approximate pattern of the individual radiator largely uncontaminated by the other competing sources of radiation.**

Keywords- near-field scanning; spherical near-field; modal filtering; antenna diagnostics.

I. INTRODUCTION

Recently, we have developed a filtering technique that provides for suppression and elimination of the effects of unwanted extraneous signals from the patterns produced in spherical near-field scanning. [1] The three successive steps in this method are first to sample (or over-sample) in the scanning data domain and transform to the far field, then to effect a translation of the coordinate origin, and lastly to filter in the domain of the spherical modal coefficients as the far-field pattern is re-computed. It is a straightforward extension of the usual spherical modal domain filtering. We have given the name "***IsoFilter***™ " to this sequence of steps.

The ***IsoFilter***™ technique allows us to apply modal filtering to any sub-sphere contained within the measurement sphere. As is well known, the increasingly higher modes correspond to increasing radius from the spherical near-field (SNF) coordinate origin. Reconstructing the pattern using only lower-order modes leaves out the interference from radiators outside that sphere which corresponds to the modal order chosen.

II. METHOD OF TRANSLATING THE ORIGIN OF THE COORDINATE SYSTEM COMPUTATIONALLY SELECTING A TEMPLATE (HEADING 2)

The method by which the coordinate origin is translated is based upon a very general theorem well known to all who have studied electromagnetics: In the asymptotic limit as the distance from a source of radiation becomes infinite, the far electric and magnetic fields separate into a product of a simple scalar function of the distance r and a vector function of direction:

$$\lim_{r \to \infty} \vec{E}(r,\theta,\phi) \;\to\; \frac{e^{ikr}}{kr}\vec{F}(\theta,\phi) \tag{1}$$

The SNF transform yields the quantity $\vec{F}(\theta, \phi)$, whose magnitude is not modified by a shift of coordinate origin. Furthermore, in the limit the amplitude factor $1/kr$ is not changed either. If we want to find the far electric field in a coordinate system that is shifted along the z-axis by a distance d_0 we have only to modify the phase factor. Please see Figure 1. The difference in the distance to the far-field sphere from the measurement origin as compared to the translated origin is simply

$$R^{FF} - R^{FF\prime} \equiv \lim_{r,\, r' \to \infty} r - r' = d_0 \cos\theta \tag{2}$$

If we substitute from this equation (2) into (1) above, making use of the relations

$$\theta' = \theta \qquad \phi' = \phi \tag{3}$$

we find we can write, in the translated coordinate system that

$$\lim_{r' \to \infty} \vec{E}(r',\theta',\phi') \;\to\; \frac{e^{ikr'}}{kr'}\vec{F}'(\theta',\phi') \tag{4}$$

where

$$\vec{F}'(\theta',\phi') = e^{ikd_0 \cos\theta'}\vec{F}(\theta',\phi') \tag{5}$$

To accomplish the translation, we simply modify the phase of each point in the far electric field by the amount corresponding to the distance appropriate for the angle θ at which that point lies.

$$\varphi^{FF\prime} = \varphi^{FF} + kd_0 \cos\theta \tag{6}$$

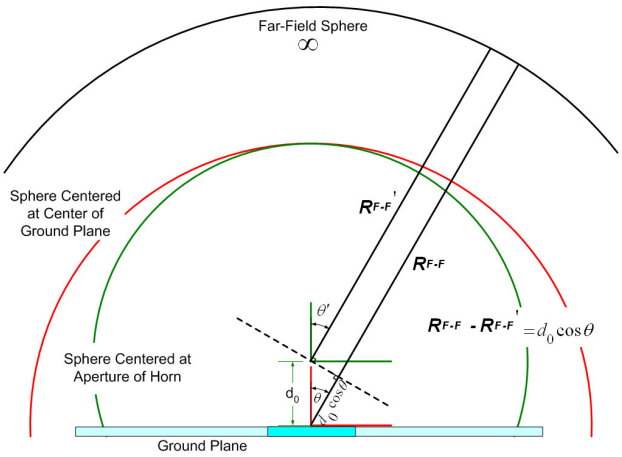

Figure 1. Schematic Illustrating Difference in Distance to Far-Field Spherical Surface from Origins of Coordinate Systems Located at Center of Ground Plane and Center of Horn Aperture

III. Chamber Simulation of Antenna Above a Ground Plane

To simulate the configuration of an antenna-above-a-ground-plane we at MI Technologies set up in a small chamber a model of this configuration. A photograph is shown below in Figure 4. A horn centered 6 inches above the ground plane is shown. The diameter of the ground plane was 36 inches. The frequency of the radiation used for these tests was 8 GHz.

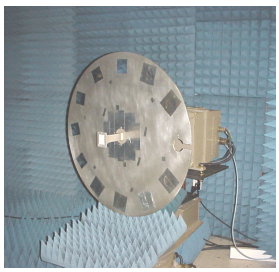

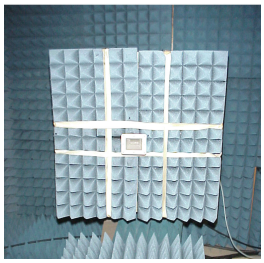

Figure 2. Photograph of Spherical Near-Field Pattern Measurement Range with a Pyramidal Horn Antenna Above a Ground

Figure 3. Photograph of the Configuration for Measurements of the Bare Pyramidal Horn Antenna Decoupled by Absorber from the Ground Plane

The result of the pattern measurement of the horn plus ground plane using the spherical near-field technique is shown in Figure 3. The broad symmetric pattern with ripples imposed by the secondary sources is immediately evident. Compare this to Figure 4, where the same cut is shown after applying the ***IsoFilter***™ technique; there the pattern appears with the interference eliminated.

When the ground plane was covered with absorber and the resulting unfiltered pattern compared to the filtered pattern with the ground plane uncovered, the agreement between the two patterns lead to our conclusion that the modal filtering is very effective at isolating the horn from the ground plane. Please see Figure 6.

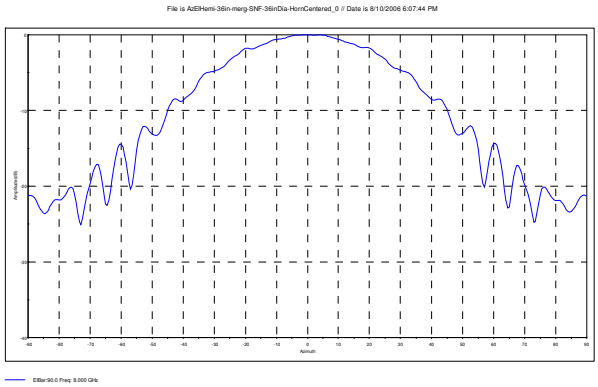

Figure 4. Azimuth Cut of Horn Mounted Above a 36 inch Diameter Ground Plane
(Scale: Vertical 40 dB; Horizontal ± 90°)

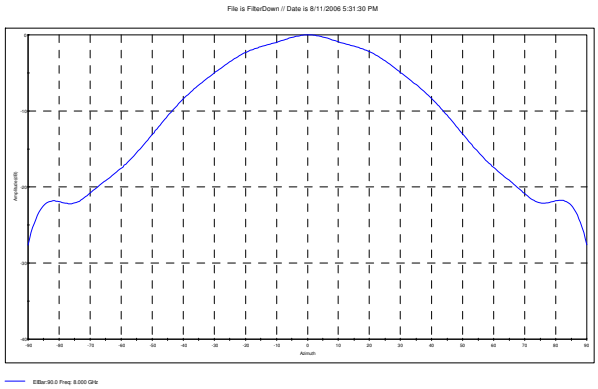

Figure 5. ***IsoFiltered***™ Azimuth Cut of Horn Mounted Above a 36 inch Diameter Ground Plane
(Scale: Vertical 40 dB; Horizontal ± 90°)

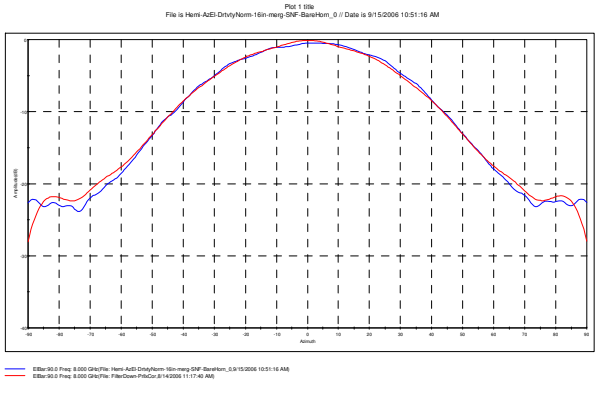

Figure 6. ***IsoFilter***™'ed Azimuth Cut of Horn Mounted Above a 36 inch Diameter Ground Plane versus Horn Mounted Above a 24 inch Square of Absorber
(Scale: Vertical 40 dB; Horizontal ± 90°)

We also applied the technique to the more difficult case of a horn mounted well off the center of the ground plane and found the technique to be similarly effective at reducing the effect of electromagnetic coupling between the radiating horn and the nearby ground plane. [2]

IV. The IsoFilter Rejection Curve

To understand better the limitations of the ***IsoFilter***™ Technique we at MI Technologies have developed and investigated the idea of the 'rejection' curve. [3]

We start with a small antenna at the origin, then apply a succession of ***IsoFilter***™ spheres whose centers progress along a coordinate axis. Once the filtering sphere no longer contains any radiating sources, any reported signal represents interference that would add to the desired signal from an antenna located inside the filtering sphere. This approach was taken using measured data.

We demonstrate with measured data an empirical procedure by which we may quantify the degree of rejection offered by the ***IsoFilter***™ method. Recall first the configuration of the spherical near-field range on which the measurements for demonstrating ***IsoFilter***™ were taken. It consisted of a roll-over-azimuth positioner with a fixed probe antenna. The pyramidal horn antenna was mounted above a ground plane, offset by 6 inches along the roll axis. The roll and azimuth axes crossed at a point that lay precisely upon the ground plane surface. Please see Figures 2 and 3 for photographs of the setup, where the horn is centered above the ground plane on the roll axis. The ground plane was covered by a panel of absorber to form a measurement configuration we refer to as the "bare horn" configuration, shown in Figure 2.

It was demonstrated earlier that the ***IsoFilter***™ technique provided a pattern measurement result of the horn above the ground plane that agreed well with the measured pattern of the bare horn. We use the bare horn pattern data taken earlier as the basis for ascertaining a quantitative measure of the degree of rejection provided by ***IsoFilter***™.

A spherical isometric plot showing the measured forward hemisphere is provided in Figure 7.

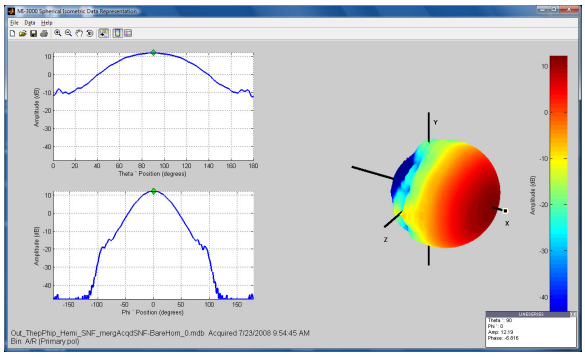

Figure 7. Spherical Isometric Plot of Forward Hemisphere of Bare Pyramidal Horn

After translating to the center of the aperture of the horn, the spherical modal distribution occupies modal bins that extend only up to modal order n = 5, for a 30 dB dynamic range as shown in the tabulation exhibited in Figure 8.

Figure 9 below illustrates the process we used to determine the ***IsoFilter***™ rejection curve for the measured horn data. The ***IsoFilter***™ sphere was translated along the X axis from 0" to 18" in 0.1" steps.

For translations large enough that the horn is no longer contained in the ***IsoFilter***™ sphere, the desired transform output should contain zero power. Any power reported in those outer spheres therefore represents imperfect rejection. If there were a source contained in a particular ***IsoFilter***™ sphere, then the signal returned by this procedure represents the intensity of that source. The sequence of translations corresponds to points along the x-axis of the measurement coordinate system, which lies in the H-plane of the horn. The data were measured at 8.0 GHz, so the 0-18" translations corresponded to approximately 0-12.2 wavelengths. This is to be compared to the 3 inch – i.e. 1½ wavelength – lateral dimension of the H-plane of the pyramidal horn.

Amount of POWER (in Watt) for each POLAR mode

N	POWER	Accumulated POWER
1	2.3479439E-01	2.3479439E-01
2	1.6614209E-01	4.0093648E-01
3	7.2364792E-02	4.7330129E-01
4	1.9712446E-02	4.9301374E-01
5	4.5521087E-03	4.9756584E-01

Figure 8. Summary Tabulation of Accumulated Power in Spherical Modes for Bare Horn with Origin Centered at Aperture

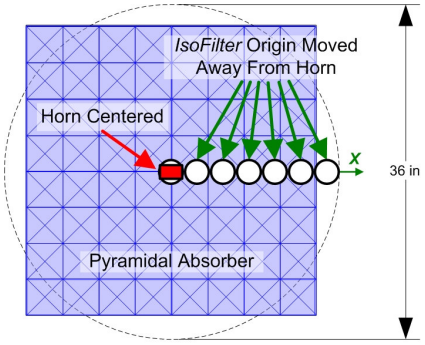

Figure 9. Locus of Points Where ***IsoFilter***™ Rejection Was Evaluated

The ***IsoFilter***™ technique was applied over and over in steps of 0.1", and the level of the accumulated power in spherical modes corresponding to modal orders 1 through 5 was plotted as a function of translation distance. The result is shown in Figure 10. Of most interest is the case for n=1.

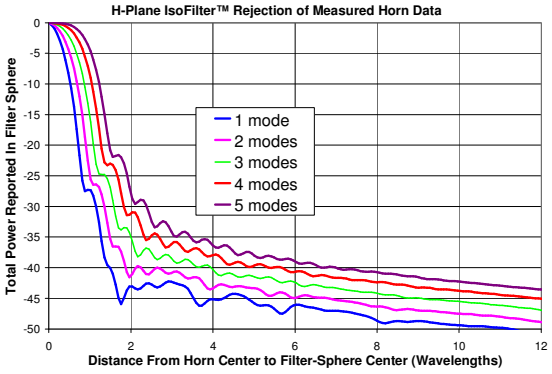

Figure 10. ***IsoFilter***™ Rejection of Measured Horn Along x-Axis. Plot of Normalized Total Power versus Radial Distance of Filter Sphere from Center

V. THEORETICAL DESCRIPTION OF REJECTION CURVE AND APPLICATION TO ANTENNA DIAGNOSTICS

Beginning with the standard expression for computing the electric field outside the region containing a set of sources, we find the well-known expression for calculating the electric field as a sum over vector modes. [4], [5] In the language of the spherical near-field scanning literature, one may write for the electric field outside the source region as a sum of complex coefficients $Q^{(3)}_{smn}$ and outgoing spherical vector modes $\vec{F}^{(3)}_{smn}(\vec{r})$:

$$\vec{E}(\vec{r}) \approx \sum_{smn} Q^{(3)}_{smn} \vec{F}^{(3)}_{smn}(\vec{r}) \quad . \tag{7}$$

This equation underlies all of spherical near-field scanning.

In his Appendix A1.5, Hansen shows how one may utilize the reciprocity theorem to obtain from the current distribution(s) an expression for these expansion coefficients, Q_{smn}. [5] The result is

$$Q_{smn} = (-)^{m+1} \iiint_V \Big(\frac{k}{\sqrt{\eta}} \vec{F}^{(1)}_{s,-m,n}(\vec{r}) \cdot \vec{J}(\vec{r}) + ik\sqrt{\eta}\, \vec{F}^{(1)}_{3-s,-m,n}(\vec{r}) \cdot \vec{M}(\vec{r}) \Big) dV \quad . \tag{8}$$

Note that this is a spatial integral over a spherical volume. If one knows the mathematical form of the prescribed current distribution(s), then the expansion coefficients may be computed from this equation.

Interpretation of this equation may be pursued from a knowledge of the form of the two types of vector wave functions that are used in the expansion. Hansen's spherical wave functions are simply the Stratton spherical wave functions, made into complex functions by allowing m to take on both positive and negative values and renormalized in a manor unique to Hansen for spherical near-field theory.

Direct evaluation of the integrals in equation (8) to obtain the Q_{smn} is difficult in general. One may gain some insight into the trend as n increases toward larger and larger values by examining the behavior of the radial parts of the spherical functions. In cases where the current sources are strongest at some distance from the origin, one generally would expect the Q_{smn} to peak once the maxima of the radial functions approach the region of strength. Rather than looking at this behavior in detail, we proceed with an heuristic alternative.

We now define an effective current which concentrates the average value at the origin

$$\vec{J}^{\,Eff}(\vec{r}') \equiv \vec{J}^{\,Ave}\, V\, \delta(\vec{r}') \quad . \tag{9}$$

Continuing to evaluate equation (8) we choose to neglect the possibility of magnetic sources being used in the modeling and rewrite (8) as follows with the help of (9). Please see equation (10) which evaluates to zero except when s=2, n=1; there are only three non-zero coefficients Q_{smn}, corresponding to m= -1, 0, +1.

$$\begin{aligned} Q_{s,-m,n} &= (-)^{m+1} \frac{k}{\sqrt{\eta}} \iiint_V \vec{F}^{(1)}_{s,m,n}(\vec{r}') \cdot \vec{J}^{\,Eff}(\vec{r}')\, dv' \\ &= [\,(-)^{m+1} \frac{k}{\sqrt{\eta}} \vec{J}^{\,Ave}\,] \iiint_V \vec{F}^{(1)}_{s,m,n}(\vec{r}') \cdot \delta(\vec{r}')\, dv' \\ &= [\,(-)^{m+1} \frac{k}{\sqrt{\eta}} \vec{J}^{\,Ave}\,]\; \vec{F}^{(1)}_{s,m,n}(0) \end{aligned} \quad . \tag{10}$$

From Hansen's Appendix, A1.5, equation (18) above which is expressed in spherical coordinates may also be expressed in Cartesian coordinates:

$$\begin{aligned} \vec{F}_{211}(0,\theta,\phi) &= \frac{\sqrt{3}}{6\sqrt{\pi}}(\hat{x} + i\hat{y}) \\ \vec{F}_{201}(0,\theta,\phi) &= \frac{\sqrt{6}}{6\sqrt{\pi}}(\hat{z}) \\ \vec{F}_{2-11}(0,\theta,\phi) &= \frac{\sqrt{3}}{6\sqrt{\pi}}(\hat{x} - i\hat{y}) \end{aligned} \tag{11}$$

Thus the only non-zero coefficients, for s=2; n=1, and m= -1, 0, +1.

$$\begin{aligned} Q_{2,-1,1} &= [\,\frac{k}{\sqrt{\eta}} \frac{\sqrt{3}}{6\sqrt{\pi}}\,]\; \vec{J}^{\,Ave} \cdot (\hat{x} + i\hat{y}) \\ Q_{2,0,1} &= [\,\frac{k}{\sqrt{\eta}} \frac{\sqrt{6}}{6\sqrt{\pi}}\,]\; \vec{J}^{\,Ave} \cdot (\hat{z}) \\ Q_{2,1,1} &= [\,\frac{k}{\sqrt{\eta}} \frac{\sqrt{3}}{6\sqrt{\pi}}\,]\; \vec{J}^{\,Ave} \cdot (\hat{x} - i\hat{y}) \end{aligned} \quad . \tag{12}$$

These equations can be inverted to yield the average current values associated with the particular coordinate origin. In general they are a function of the particular origin which is varied by the use of the ***IsoFilter***™ translation, $\vec{r}_{Iso}$ so they need to be written as functionally dependent upon the location of the coordinate origin:

$$\begin{aligned} J^{Ave}_x(\vec{r}_{Iso}) &= \frac{\sqrt{\eta}}{k}\sqrt{3\pi}[Q_{2,-1,1}(\vec{r}_{Iso}) + Q_{2,1,1}(\vec{r}_{Iso})] \\ J^{Ave}_y(\vec{r}_{Iso}) &= (-i)\frac{\sqrt{\eta}}{k}\sqrt{3\pi}[Q_{2,-1,1}(\vec{r}_{Iso}) - Q_{2,1,1}(\vec{r}_{Iso})] \\ J^{Ave}_z(\vec{r}_{Iso}) &= \frac{\sqrt{\eta}}{k}\sqrt{6\pi}[Q_{2,0,1}(\vec{r}_{Iso})] \end{aligned} \tag{13}$$

This result giving the source intensity versus location (of the translated origin) can form the basis for antenna diagnostics.

REFERENCES

[1] D. W. Hess, "The ***IsoFilter***™ technique: isolating an individual radiator from spherical near-field data measured in a contaminated environment," Post-Deadline Paper, AMTA 2006, Austin TX.

[2] D. W. Hess, "The ***IsoFilter***™ technique: extension to transverse offsets," Post-Deadline Paper, AMTA 2006, Austin TX.

[3] D. W. Hess & S. McBride, "Evaluation of ***IsoFilter***™ fidelity in selected applications," AMTA Symposium Digest, pp. 289-295, Boston, MA, 2008

[4] D. W. Hess, "A theoretical description of the ***IsoFilter***™ rejection curve," AMTA Symposium Digest, pp. 161-166, Atlanta, GA, 2010.

[5] J. E. Hansen, Editor, Spherical Near-Field Antenna Measurements, Peter Peregrinus, Ltd., London, U.K., 1988.